Received: 1 February 2022 | Revised: 12 September 2022 | Accepted: 16 September 2022

DOI: 10.1002/hyp.14708

RESEARCH ARTICLE

WILEY

Riparian zone as a variable source area for the estimation of evapotranspiration through the analysis of daily fluctuations in streamflow

Muhammad Waqas Sarwar[1] | David I. Campbell[2] | Ali Shokri[1]

[1]School of Engineering, University of Waikato, Hamilton, New Zealand

[2]School of Science and Environmental Research Institute, University of Waikato, Hamilton, New Zealand

Correspondence
Ali Shokri, School of Engineering, University of Waikato, Private Bag 3105, Hamilton 3240, New Zealand.
Email: ali.shokri@waikato.ac.nz

Abstract

Evapotranspiration is a critical component of the water balance of a catchment, and riparian zones play a crucial role in the hydrological process. However, the influence of riparian zones on evapotranspiration, especially at a catchment scale, needs more investigation. Since evapotranspiration is negligible at night, the difference in recharge between day and night generates diurnal fluctuations in streamflows. A new method is developed to estimate riparian evapotranspiration by analysing the streamflow response to diurnal evapotranspiration. The potential evapotranspiration (PET) calculated by FAO-56 is used as a true reference for validation. The estimated evapotranspiration shows acceptable goodness of fit with the hourly PET calculated from FAO 56. However, the new approach estimates average evapotranspiration across the entire riparian area than a point observation and provides a better understanding of the impact of the riparian zone on streamflow patterns.

KEYWORDS
baseflow, diurnal signals, evapotranspiration, riparian zone, streamflow daily fluctuations

1 | INTRODUCTION

For many decades, studying the impact of evapotranspiration (ET) on the hydrological process of a catchment has been a challenge (Gribovszki, Kalicz, et al., 2008; Troxell, 1936). Particularly in riparian zones with a shallow water table and a heterogeneous environment. In this region, plant roots have immediate access to groundwater resources, and ET may impact the water table and streamflow significantly (Kellogg et al., 2008; Satchithanantham et al., 2017).

The riparian zone is often defined as part of the landscape along the boundaries of a water body (Rugenski et al., 2017). Often part of riparian zones that are fully saturated and directly influence the outflow patterns are known as active riparian zones (Barnard et al., 2010). However, there is a diverse interpretation of the definition and size of an active riparian zone in the literature, and the scientific and applied literature can be confusing due to the variety of terms used Dufour and Rodríguez-González (2019). The active riparian zone is sometimes defined as a fixed width from the stream network. For example, Reigner (1966) indicates that an area of up to 2 m from the stream is the riparian zone, as this area has a considerable impact on streamflow. Geisler (2016), on the other hand, suggests that the area adjacent to the stream with a slope of less than 25° is the riparian area. Figure 1 shows an interpretation of the riparian zone by Reigner (1966) and Geisler (2016). Still, these suggestions conflict with the findings of some experimental studies that report the riparian area shrinks gradually as the catchment dries out (Barnard et al., 2010; Graham et al., 2012; Tschinkel, 1963). Dufour and Rodríguez-González (2019) provided comprehensive literature for

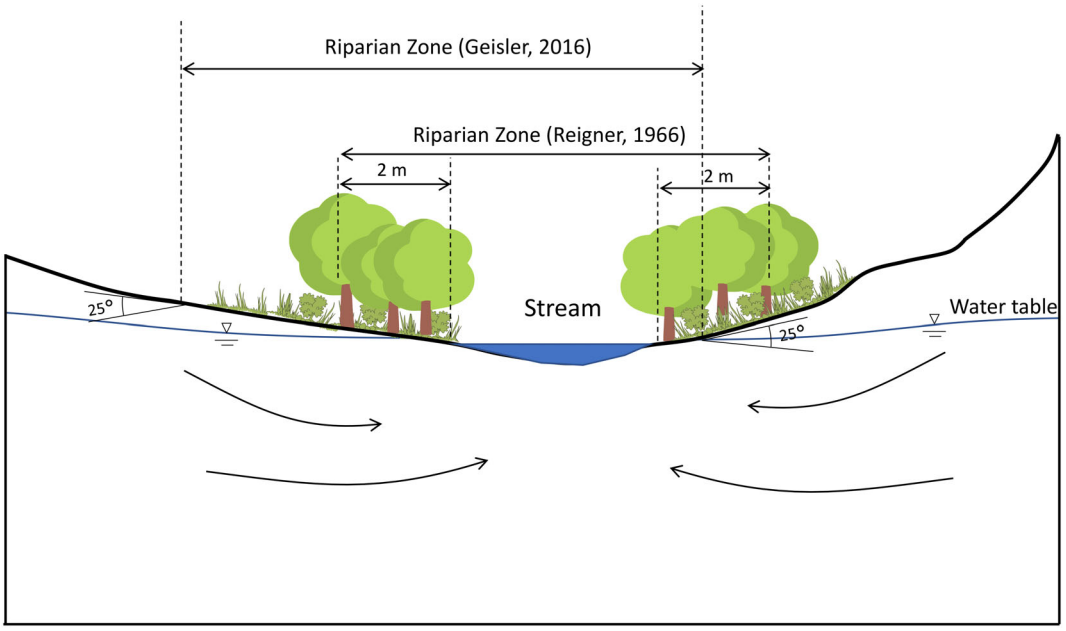

FIGURE 1 A schematic diagram of a riparian zone along the stream banks and a diverse interpretation of the definition and size of an active riparian zone.

definitions of the riparian zone. For clarification in this paper, the active riparian zone refers to a saturated/unsaturated region that is hydrologically connected with the stream and directly influences flow.

Characteristics of the soil and vegetation in the active riparian area are different from the surrounding landscape due to their vicinity to the water resources. Riparian zones are also important from a hydrological point of view, as the riparian storage connects the hillslope groundwater reservoir and the water bodies. Consequently, the riparian zone significantly impacts streamflow more than the rest of the catchment (Johnson et al., 2013; Martí et al., 2000).

Since riparian zones have an adequate water supply throughout the year, these zones are critical to the ET process, particularly during the dry summers (Johnson et al., 2013). Thus, studying the influence of ET on riparian zone and consequently on the water table and streamflow can reveal critical information on vegetation-stream interactions in headwater catchments, where ET of riparian has a significant effect on stream flow (Széles et al., 2018). Nevertheless, several challenges for estimating ET from riparian zones are indicated in the previous studies. For example, the narrow width of the riparian zone around a stream is likely below the fetch requirements of the eddy covariance and Bowen ratio ET measurement techniques (Goodrich et al., 2000; Nachabe et al., 2005). Also, installing lysimeters in the vegetation corridor along streams is costly and only yields point measurements.

Alternatively, Physiological methods such as crop coefficients, sap flow, and leaf chamber systems are highly effective in determining ET rates using simple techniques at a relatively low cost (Lascano et al., 2016). However, when there is a degree of non-homogeneity in the vegetation and soil types, the physiological methods are ineffective (Goodrich et al., 2000). Hence, remote sensing techniques are employed to estimate the ET distribution (Brunner et al., 2008).

On the other hand, the day and night variation in solar radiation leads to diel fluctuation in ET (Széles et al., 2018). These daily changes in ET cause a periodic depletion and replenishment of groundwater from riparian vegetation, which impacts the discharge and produces daily fluctuations in streamflow (Bond et al., 2002; Burt, 1979; Graham et al., 2012; Gribovszki et al., 2010; Lundquist & Cayan, 2002; Schwab et al., 2016). ET-induced diurnal fluctuations are often characterized by a local maximum in the early morning followed by a local minimum in the afternoon. The daily fluctuations in the water table, soil moisture and streamflow in response to higher ET during the daytime show potential for ET estimation (Dolan et al., 1984; Troxell, 1936; White, 1932).

White (White, 1932) was the first who established a method for estimating ET from daily water table fluctuations. He used a uniform recovery rate over 24 h to calculate the total volume of water evaporated due to diurnal water table fluctuations. To date, the White method has received extensive modifications (Fahle & Dietrich, 2014; Gribovszki, Kalicz, et al., 2008; Loheide II, 2008; Nachabe et al., 2005; Szilagyi et al., 2007). However, the high spatiotemporal variability of groundwater recharge and specific yield remain the primary challenge of the White method (Fahle & Dietrich, 2014).

The analysis of daily fluctuations in streamflow in the absence of rainfall during a flood recession is also a practical and cost-effective way of characterizing catchment hydrological processes (Lundquist & Cayan, 2002; Széles et al., 2018). Some studies used the diel fluctuations in streamflow to estimate riparian zone ET (ET_r). Troxell (1936) and Boronina et al. (2005) estimated ET_r using a similar approach to the White method by assuming a constant recharge and computing the daily flow deficit caused by ET during a flood recession. Loheide II (2008), on the other hand, developed an empirical relation based on

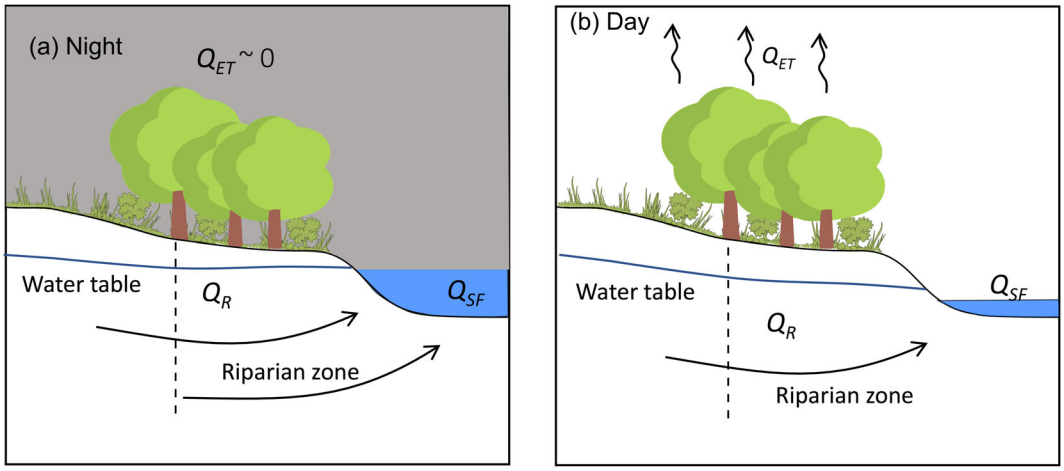

FIGURE 2 A conceptual cross-section of a riparian zone and water balance components that contribute to streamflow during (a) night and (b) day.

the rate of change of groundwater level during the periods of zero ET at night to include the change in recharge between days and nights. Later, Cadol et al. (2012) modified an empirical relation for estimating ET from streamflow fluctuations by combining the empirical equation developed by Loheide II (2008) with the daily streamflow deficit. However, uncertainties in identifying specific yields and groundwater recharge for each night made these methods less practicable (Fahle & Dietrich, 2014). In addition, some studies show that the riparian zone and vegetations in streams play a dominant role in producing and controlling the diel fluctuations in streamflow (Barnard et al., 2010; Bond et al., 2002; Graham et al., 2012). However, the relationship between ET and the riparian size for generating daily signals in streamflow has been widely neglected in previous studies.

Therefore, the main aim of this study is to analyse the daily streamflow fluctuations to estimate hourly and daily riparian ET while evaluating the area of the riparian area around stream networks in a headwater catchment. The new approach emphasizes the interconnection between ET and the riparian zone to quantify the relationship between ET and daily streamflow fluctuations and investigate how changes in the riparian area affect ET loss.

2 | METHODS

2.1 | Calculation of riparian ET (ETr)

A conceptual cross-section of a riparian zone is illustrated in Figure 2. In the absence of rainfall during a flood recession, the riparian water balance can be written as:

$$Q_R - Q_{Sf} - Q_{ET} = \frac{dV}{dt} \quad (1)$$

where Q_R is the groundwater recharge, Q_{sf} is the observed streamflow at the outlet, Q_{ET} is the ET flow abstract, $\frac{dV}{dt}$ is the water storage change in the riparian zone. Groundwater recharge can be influenced by many factors, such as the difference in water level between the river and groundwater, the hydraulic conductivity of the riverbed, and changes in the groundwater recharge boundary (Brunner et al., 2009). Since ET is negligible during nights, groundwater recharge is the only source of flow in streams. Therefore, the difference in recharge between day and night results in a diurnal streamflow fluctuation.

Previous studies report a lag time (t_{lag}) between the maximum ET in the catchment and minimum streamflow at the outlet for each diurnal fluctuation. For example, the maximum ET is observed between 12 PM and 3 PM, and the minimum flow is between 5 PM and 8 AM (Kirchner, 2009; Szilagyi et al., 2007; Troxell, 1936). The lag time is reported to be varied seasonally due to changes in the flow paths and flow velocities (Barnard et al., 2010; Cadol et al., 2012). Also, it is suggested that the lag time can be resulted from the riparian system's dynamical lag to integrate the effects of its sinusoidal inputs into outputs over time(Kirchner et al., 2020).

In this study, a similar approach suggested by Gribovszki, Kalicz, et al. (2008) for estimating ET from groundwater table fluctuations is adopted for streamflow fluctuations. First, a Bezier-Spline interpolation curve is fitted to the observed streamflow hydrograph in this method. Then the differences between the interpolation curve and streamflow are calculated as Q_d. An example of fitting a Bezier-Spline interpolation curve to a streamflow hydrograph is illustrated in Figure 3.

The interpolation curve is formed by linking the daily minimum and maximum discharge points at the beginning and end of the periods when the effect of ET became negligible on streamflow. Time series of ET from the active riparian area (ET_r) is obtained by:

$$ET_r(t - t_{lag}) = \frac{Q_d(t)}{A_r(t)} \quad (2)$$

where t_{lag} is the lag time between the maximum ET and minimum streamflow observed at the outlet for each fluctuation, $ET_r\ (t - t_{lag})$ is

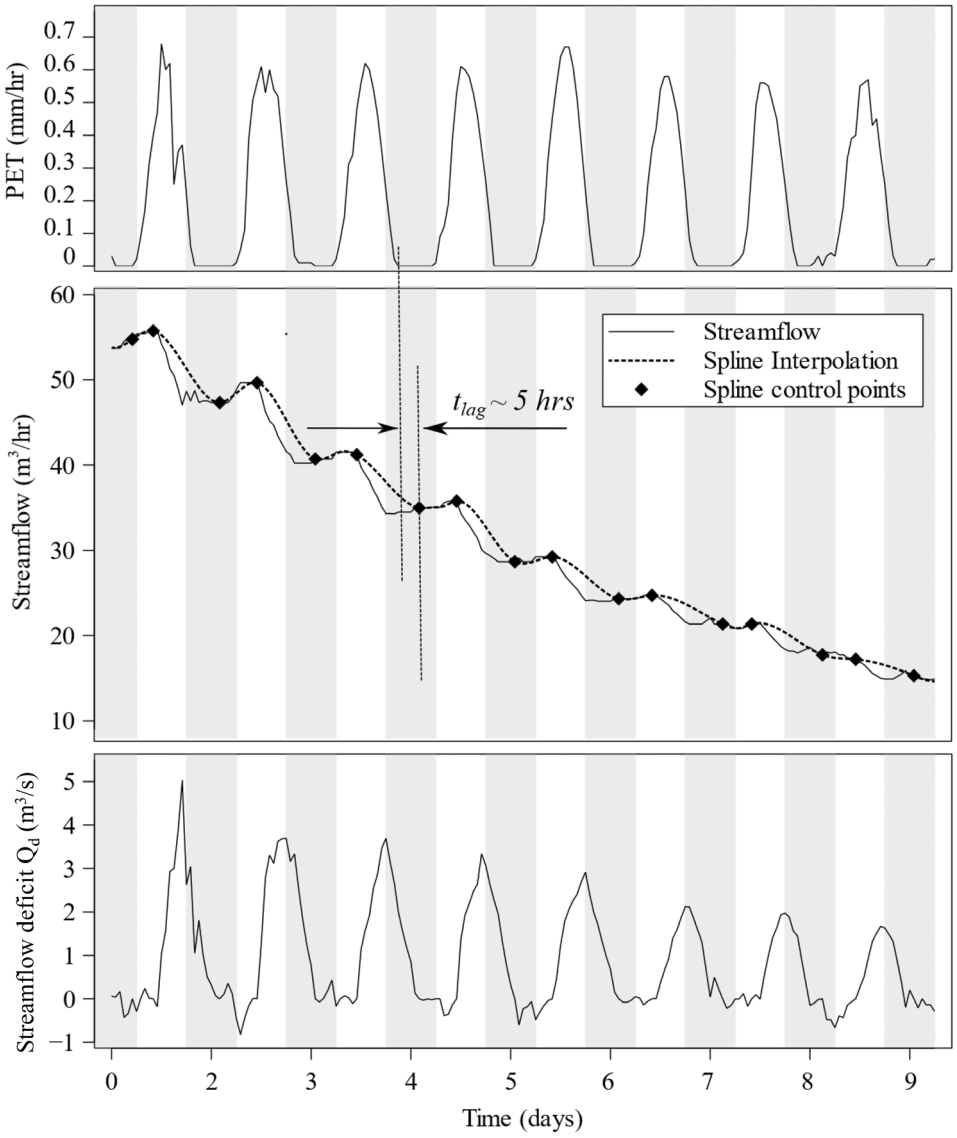

FIGURE 3 An example of fitting a Bezier-spline interpolation curve to a streamflow hydrograph, estimation of streamflow deficit Q_d and lag time t_{lag}; and a comparison with potential evapotranspiration (PET) and Q_d

the time series of average ET abstracted from the riparian area, $Q_d(t)$ is the streamflow deficit which is the difference between the interpolation curve and streamflow at the outlet, and $A_r(t)$ is the size of the riparian zone that actively contributes to the streamflow fluctuations.

2.2 | Area of the riparian zone, Ar(*t*)

It has been observed that groundwater storage in the riparian area decreases as the catchment starts to dry out (Bond et al., 2002). As a result, the active riparian zone shrinks gradually as groundwater storage reduces. Although the ET per unit area remains unchanged during the recession, the total volume of water ET loss in the riparian zone decreases slowly as the size of the riparian area decreases. A conceptual example of the shrinkage of the active riparian area around a stream network in three-time steps is illustrated in Figure 4.

An exponential expression is often used to explain the flow decline during a recession (Tallaksen, 1995).

$$Q_{Sf} = Q_0 k^t \tag{3}$$

where Q_{Sf} is the streamflow in the recession period, k is the recession constant, and Q_0 is the flow at the beginning of the recession. Q_0 is defined using a recursive digital filter-based flow separation method, that is, (Lyne & Hollick, 1979). The basic equation for the digital filter is

$$Q_{Qqf}(t) = \begin{cases} \propto Q_{qf}(t-1) + \dfrac{(1+\propto)[Q_{Sf}(t) - Q_{Sf}(t-1)]}{2} & \text{for } Q_f(t) > 0 \\ 0 & \text{otherwise} \end{cases} \tag{4}$$

where Q_{qf} is the quick flow at time t, and$\propto$ is the digital filter parameter through which the shape of the separation curve can be altered. Q_0 as the beginning of the recession period can be estimated as a point where the quick flow has become zero after a rain event. An example of estimation of Q_0 using the Lyne & Hollick digital filter is shown in Figure 5.

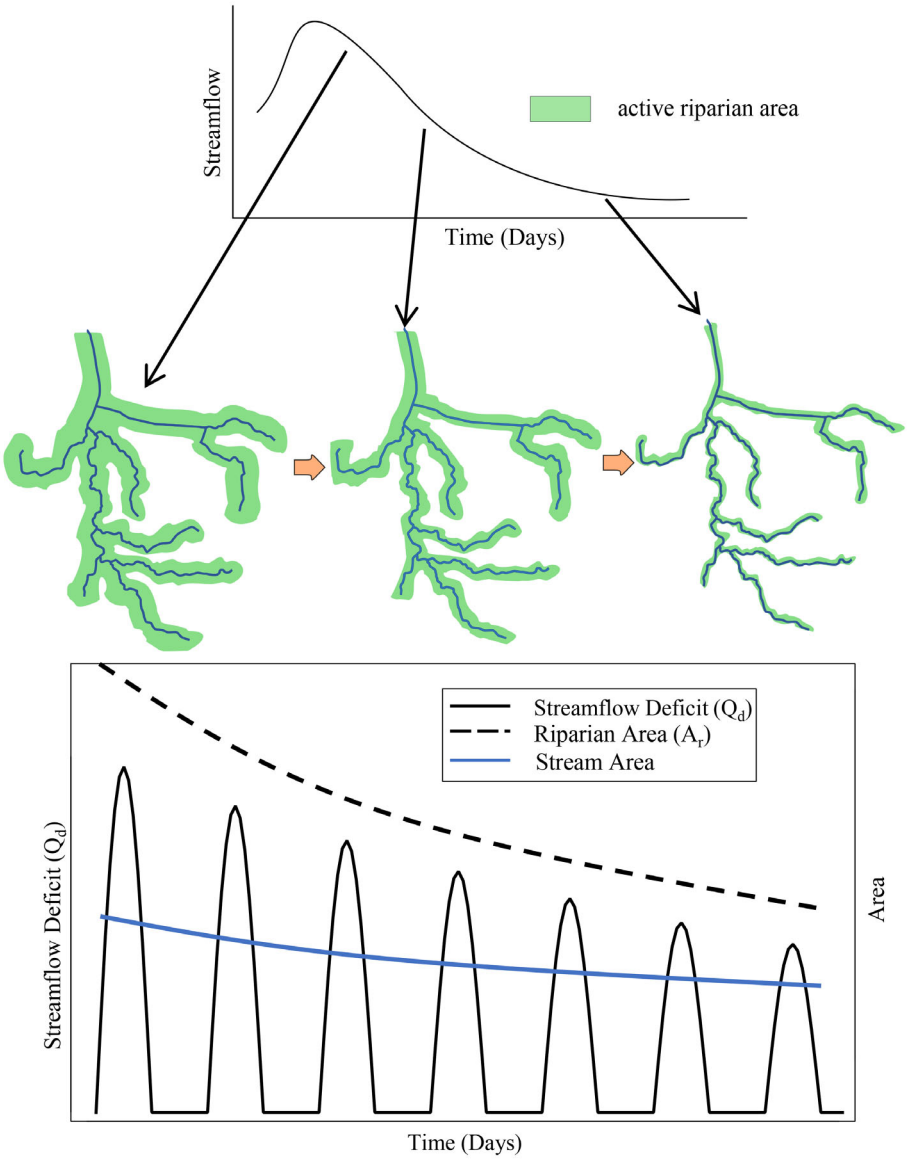

FIGURE 4 A schematic of the active riparian area around a typical stream network after a flood event in three time-steps.

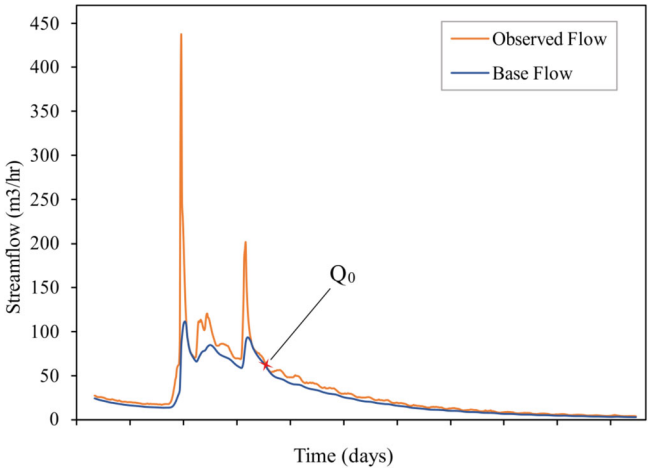

FIGURE 5 Separation of quick flow and baseflow with the Lyne & Hollick digital filter method when $\propto = 0.95$

During a flood recession, where groundwater recharge is the only resource and ET is the sole abstracting agent, the area of the active riparian zone may have linear, exponential, power, and so forth, relationships with the streamflow rate during a recession period (Fenicia et al., 2006; Spence & Mengistu, 2019). In this study, a simple linear relationship is assumed. However, this assumption can be modified if other correlations are desired. Therefore, the area of the riparian zone is assumed to be directly proportional to the streamflow rate:

$$A_r(t) = A_0 k^t \tag{5}$$

where A_0 is the initial active riparian area at the beginning of the recession.

Combining equations 3 and 5 yields:

$$A_r = \frac{A_0}{Q_0} Q_{SF} \tag{6}$$

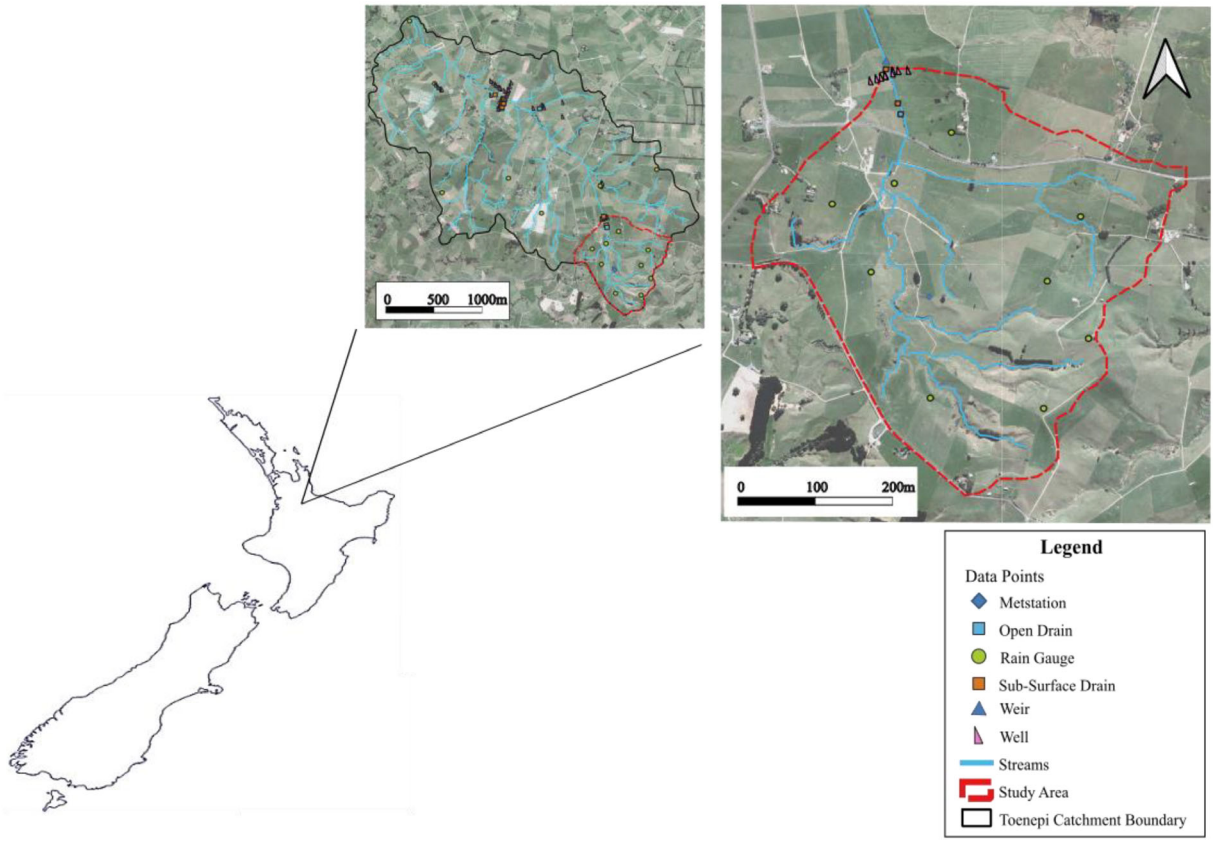

FIGURE 6 The Toenepi catchment and the study area boundary

Then, combining Equations (2) and (6) yields:

$$ET_r(t - t_{lag}) = \frac{Q_0 Q_d(t)}{A_0 Q_{SF}(t)} \quad (7)$$

Equation (7) hereafter is the "new method" for estimating a time series of average ET abstracted from the active riparian area (ET_r). It should be noted that Equations (5)–(7) are developed based on the assumption that a linear correlation exists between the riparian area's size and the river flow. However, for the cases where the relationship is not linear, equations 5 to 7 need to be modified to reflect the non-linear relationships.

3 | MATERIALS

3.1 | Study area

The Toenepi stream (WGS84 coordinates: −37.7146, 175.5632) drains a small catchment in the Waikato region, New Zealand (Figure 6). The catchment has an area of 1.6 ha and an elevation range from 40 to 130 m above mean sea level. The catchment is one of the five representative dairy focus catchments in New Zealand, with a good record of hydrological data available (Wilcock et al., 2006). The ground surface topography is primarily flat (max slope 6.5%) and fully covered by pasture apart from the riparian plantings around the Toenepi stream, which mainly consist of shading trees and shrubs (Wilcock et al., 2006). The vicinity of the stream comprises poorly drained Topehaehae soils (clay texture with fine loamy topsoil) (13%) developed from recent alluvium on river flood plains, 47% freely drained Kereone (sandy loam texture) and Kiwitahi soils (silty loam texture), and 40% of Morrinsville ash soils (clay texture) (Müller et al., 2010). The catchment receives an annual average rainfall of 1160 mm with an estimated ET of 892 mm/year (2003–2012), which gives a yearly water yield of around 399 mm/year (Woodward et al., 2013).

3.2 | Data access

The streamflow is monitored continuously from 1995 to 2014 at 15-min resolution, using a V-notch weir at the outlet (Wilcock et al., 2006). For this study, the available 15-min streamflow is converted to hourly values to be unified with the other meteorological data obtained from the weather station located in the study area. Then hourly PET time series are calculated using the FAO-56 Penman-Monteith method (Allen & Pereira, 1991).

$$PET = \frac{0.408\Delta(R_n - G) + \gamma \frac{900}{T+273} u_2 (e_s - e_a)}{\Delta + \gamma(1 + 0.34u_2)} \quad (8)$$

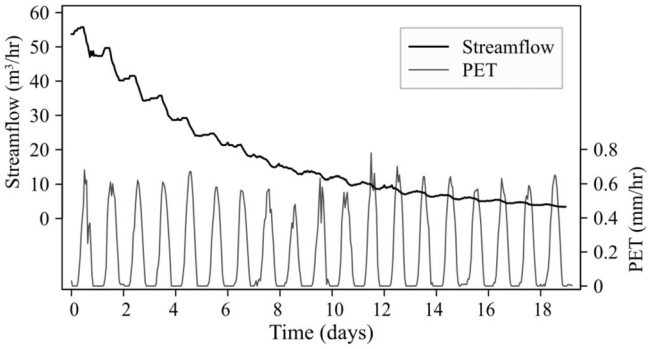

FIGURE 7 Daily flow fluctuations in Toenepi stream in response to temporal variations in ET from 12 January 2005 to 30 January 2005

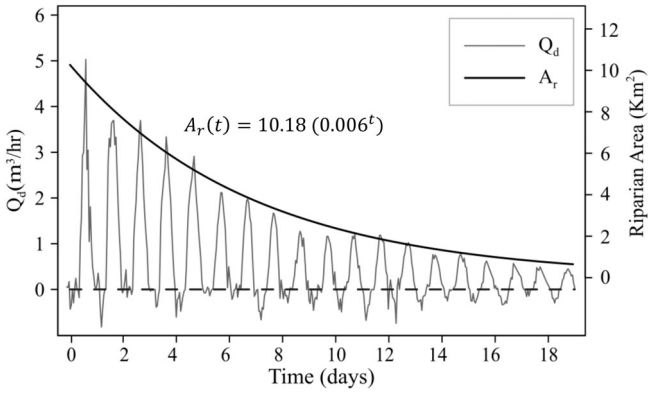

FIGURE 8 An hourly time series of *Qd* and hourly time series of riparian area (A_r) in Toenepi stream from a flood recession period between 12 January 2005 and 30 January 2005

where R_n is the net radiation at the crop surface, G is the soil heat flux density, T is the air temperature at 2 m height, γ is the psychrometric constant, u_2 is the wind speed at 2 m height, e_s is the saturation vapour pressure, e_a is the actual vapour pressure and Δ is the slope of the saturation vapour pressure curve.

4 | RESULTS AND DISCUSSION

The hourly streamflow data from 2003 to 2013 are analysed to detect the diel fluctuations. Sub-daily very small and sudden changes in flow during the flood recession curves are ignored as it is assumed they result from local and small rain events that did not impact the entire recession curves. The end of fluctuation episodes happens either the recession is interrupted by a rain event or the flow rate becomes too low to carry any signal.

A total of 40 flood recessions with at least 4 days of fluctuations are detected. The duration of the flood recessions is usually longer in warmer months, as they are less likely to be interrupted by any precipitation. Noticeable diurnal fluctuations started from late winter in August, dominated in spring (September–November) and summer (December–February) and diminished around early autumn in March. No flood recession was observed between April and July that meets the required criteria. This is likely because the ET-induced streamflow fluctuation area is a summer phenomenon, and the recession curves are interrupted by frequent rainfall during winter.

As an example, Figure 7 shows the most extended fluctuation event from 12 January 2005 to 31 January 2005, where a streamflow recession with daily fluctuations is observed for 19 days before it is interrupted by a rainstorm. During this flood recession, the PET started at around 6 AM, reached a maximum value at around noon, and dropped to zero shortly after 7 PM. A lag time of 5 h is observed between the PET and streamflow deficit Q_d peaks.

4.1 | Calculation of ET_r

The time series of Q_d (the difference between the interpolation curve and streamflow) is calculated by fitting Bezier-Spline interpolation curves to flood recessions. As an example, an hourly time series of Q_d for the recession curve from 12 January 2005 to 30 January 2005 is illustrated in Figure 8. The magnitude of Q_d declines as the average daily discharge decrease during the flood recession. Sometimes, Q_d value becomes negative during the night when the spline curve does not follow a sharp change in the actual recharge rate at the start and end of the night. The negative Q_d values are removed from the Q_d time series.

Pronger et al. (Pronger et al., 2016) suggested that the PET calculated from FAO-56 method is an appropriate reference for estimating actual ET in pasture systems in the study area. Scotter and Heng (2003) suggest that most pastures in New Zealand behave like the reference crop for most of the year. In addition, considering the majority of vegetations in the riparian area have access to adequate groundwater resources and water fluxes, PET reasonably well estimates the actual ET in the riparian zone (Loheide et al., 2005).

Therefore, it is assumed PET truly represents actual ET in the study area. The hourly time series of ET_r is calculated by minimizing the root-mean-square error between PET and ET_r calculated from Equation (7) by varying A_0 as a changing variable in the MS Excel solver.

The goodness of fit measure suggested by Kling-Gupta efficiency (KGE) (Gupta et al., 2009) is used to measure the correlation between PET and ET_r.

$$\mathrm{KGE} = 1 - \sqrt{(r-1)^2 + \left(\frac{\mu_{PET}}{\mu_{ET_r}} - 1\right)^2 + \left(\frac{\sigma_{PET}}{\sigma_{ET_r}} - 1\right)^2} \qquad (9)$$

where r is the Pearson's correlation between PET and ET_r, μ_{PET} is the mean of PET, μ_{ET_r} is the mean of ET_r, σ_{PET} is the standard deviation of PET and σ_{ET_r} is the standard deviation of ET_r. KGE ranges between 0 and 1, where 0 means no correlation and 1 represents a perfect correlation.

The estimated ET_r with and without considering 5 h lag time are compared with PET and shown in Figure 9a. The correlation is not strong when the lag time is neglected. However, by offsetting the ET_r values by 5 h, a clear relationship appears in Figure 9b.

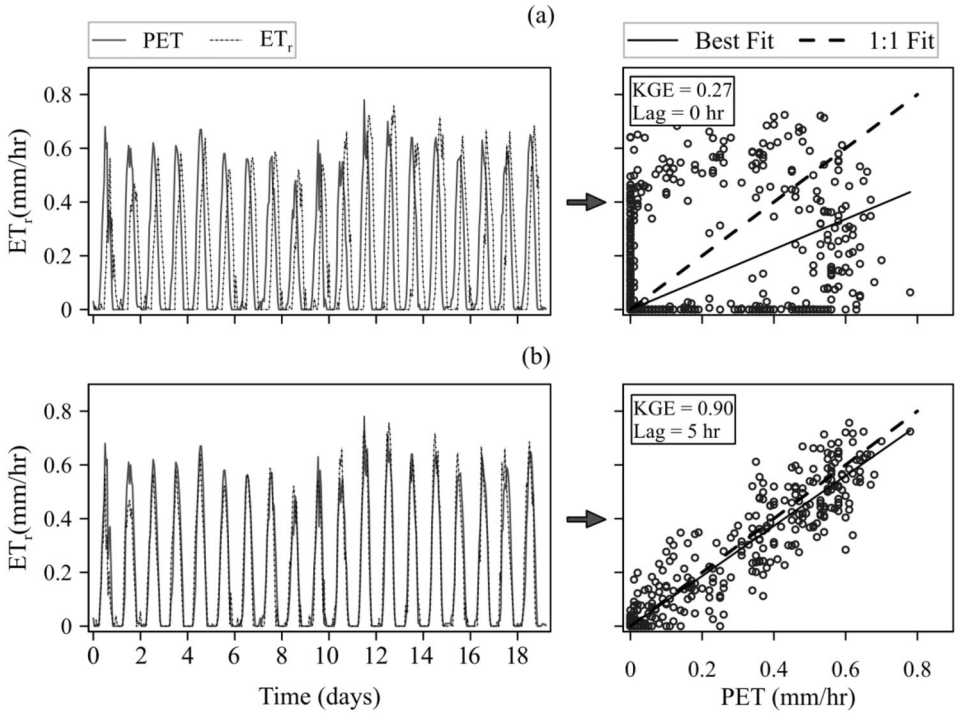

FIGURE 9 A comparison between hourly time series of PET and ET_r (a) without lag time, (b) with 5 h lag time for 19 days flood recession period between 12 January 2005 and 30 January 2005.

Practically, the best lag time between maximum PET and ET_r is estimated by offsetting the estimated ET_r by a 1-h increment for a few time steps and calculating KGE values between PET and ET_r for each time step. Ultimately, the lag time that results in the highest KGE value is considered the best lag time between PET and Q_d.

The recession constant (k) is calculated as 0.006 by fitting Equation 3 to hourly streamflow for each recession episode and A_0 as 10.18 km^2 from the minimizing the root-mean-square error between PET and ET_r. Figure 8 illustrates the hourly time series of the riparian area (A_r) estimated by substituting A_0 and k values in Equation (5). Ultimately, a comparison between the time series of A_r and Q_d indicates that the diel signal amplitude is directly proportional to the size of the riparian area.

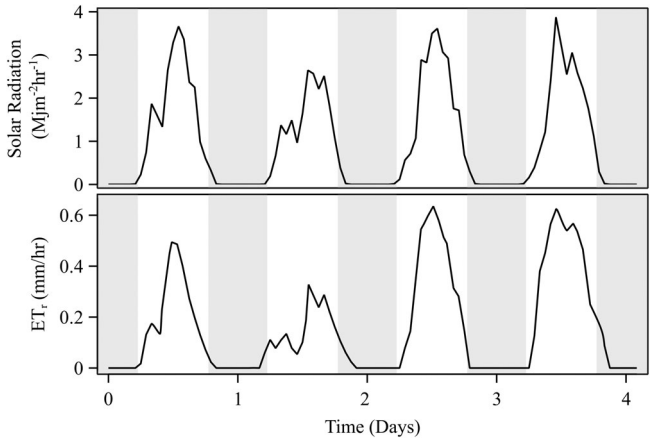

FIGURE 10 Analysing the impact of solar radiation on PET and ET_r.

4.2 | Analysis of hourly time series of ET_r

Hourly estimates of PET and ET_r for 40 flood recessions are calculated, along with the goodness of fit (KGE) and lag time illustrated in Appendices A, B and C (Figures A1, A2, and A3).

Overall, the new method shows an acceptable performance in estimating the hourly time series of ET_r compared to PET. For example, the goodness of fit (KGE) average for all flood recessions events is 0.83. However, a better correlation between ET_r and PET is observed when there are fewer variations in solar radiations during the day, and PET has a simple bell shape graph. For example, in a spring event from 5 September 2009 to 9 September 2009, the goodness of fit between PET and the new method is 0.96. On the other hand, when solar radiation frequently changes, the correlation between PET and ET_r declines.

Also, a reasonable correlation can be observed between ET_r and solar radiation. Figure 10 compares the hourly solar radiations with the diurnal signals in streamflow. It shows that the change in radiation due to temporary cloud cover impacts the diurnal signals in streamflow. This impact is more recognizable in spring and early summer events.

4.3 | Seasonal variation of ET_r

The average daily ET_r and PET for all events are calculated and compared as a scatterplot in Figure 11. Also, the seasonal breakdown of the average values of the PET and the estimated ET_r, along with the

statistical model evaluation performance, are provided in Table 1. The summer season is further divided into high (more than 1 m^3/s) and low flows (less than 1 m^3/s) to indicate the difference in properties of high and low flow diel fluctuations.

The summer events show a higher average daily ET_r, around 3.5 (mm/day), and winter events are the lowest at around 0.83 (mm/day). In autumn and spring events, the average daily ET_r ranges from 1.5 to 4 (mm/day). The scatterplot shows a good agreement between average daily PET and *ETr* with a goodness of fit of (KGE = 0.88). However, comparing a linear trendline to all events with a 1:1 line shows that daily average ET_r is marginally lower than PET. This may be due to one of two reasons. First, the spline method calculates ET_r based on the volume of the missing flow. Therefore, if the amplitude of the diel signal is reduced as it travels from the riparian zone to the stream, it could result in a lower estimated ET_r. Second, the active riparian area might be smaller than the calculated in this linear riparian reservoir method, which in turn, the model increases ET_r to balance the results.

The average of the maximum active riparian area (A_0) is calculated as 3% of the catchment area for all events. However, spring and winter events show a higher percentage of the area contributing to the diel fluctuations than summer and early autumn. Moreover, summer and early autumn had more low flow fluctuations as compared to spring and winter. This is due to the drier conditions in the former seasons, where only a very small portion of the riparian zone is active and contributing to streamflow fluctuations.

Overall, the new method shows an acceptable performance in estimating the hourly time series of ET_r compared to PET. For example, the average goodness of fit (KGE) for all flood recessions events is 0.83. However, a better correlation is observed when there are fewer variations in solar radiations during the day, and PET has a simple bell shape graph. For example, in a spring event from 5 September 2009 to 9 September 2009, the goodness of fit between PET and the new method is 0.96. On the other hand, when solar radiation frequently changes, the correlation between PET and ET_r declines. This may be because the footprint of solar radiation on ET_r is more recognizable in spring and early summer events. Also, there is a weak connotation between cloudiness and daily streamflow variability in summer, where the moisture conditions are dry and minor variations in diel signals cannot transfer to streamflow (Sumargo & Cayan, 2018).

4.4 | Seasonal variation of lag-times

The lag time is calculated for all recession episodes. A summary of seasonal variation of the lag time between ET_r and streamflow

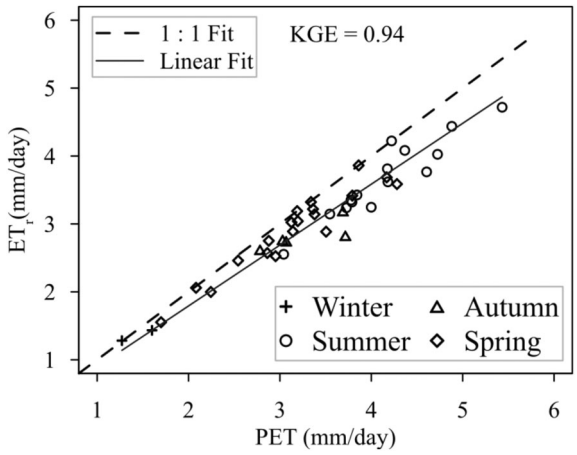

FIGURE 11 Seasonal comparison of daily average PET and ET_r

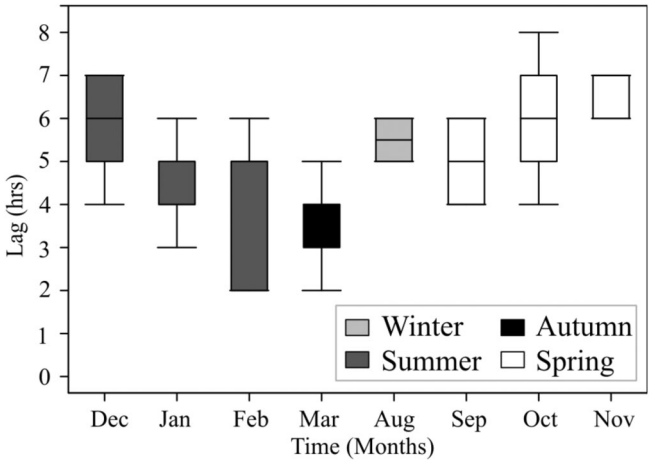

FIGURE 12 Seasonal variation in the lag time t_0 between ET_r and streamflow response in the Toenepi stream from 2003 to 2013.

TABLE 1 Seasonal breakdown of the average PET and ET_r, along with the statistical model evaluation performance.

Seasons	Daily PET mm/day	Daily ET_r mm/day	A_0 %	Q_0 m3/h	t_{lag} Hours	Bias %	Daily RMSE	KGE	R^2
Autumn (March)	2.81	2.65	0.5%	5.29	2.80	7.5%	1.00	0.68	0.58
Spring	2.94	2.51	4.0%	55.36	5.33	6.9%	0.65	0.77	0.69
Summer	4.00	3.64	3.8%	41.58	5.50	8.7%	1.10	0.81	0.73
Summer (low flew)	4.02	3.47	0.5%	1.73	2.33	12.7%	1.11	0.70	0.62
Winter (August)	1.03	0.83	6.3%	73.53	5.50	5.1%	0.20	0.74	0.66
Grand average	3.23	2.99	3%	41.85	4.85	7.9%	0.84	0.76	0.68

response is illustrated in the Toenepi stream from 2003 to 2013 Figure 12.

On average, in 40 cases, the lag time is 4.86 h, with a standard deviation of 1.47 h. It is observed that the lag time (t_{lag}) and the streamflow deficit (Q_d) vary seasonally. The average lag time is slightly shorter in spring (5.3 h) than in summer (5.52 h), but the active riparian area associated with the time lag is larger in spring than in summer.

There could be a few explanations for this seasonal variation of lag time. One explanation for the seasonal variation is that the seasonal change in vegetation in streams results in varying the roughness of the stream networks changing flow paths and baseflow velocities (Bond et al., 2002; Graham et al., 2012) and, consequently, the lag time. Also, at the beginning of spring, there is an increase in temperature and vegetation activities. In addition, soil moisture and groundwater storage are larger in spring than in summer. Therefore, a larger portion of the riparian vegetation can tap into groundwater, creating a local depression in the groundwater table. The diel fluctuations thus produced are then able to move toward stream more quickly due to well-connected pore spaces. Therefore, the water movement through the flow paths involved is relatively fast.

On the contrary, the low flow fluctuations in summers could be due to the high summer ET demand, which causes groundwater levels to drop quickly following a precipitation event. Only the plants very close to the stream can trap the stream base flow to transpire. Moreover, the falling groundwater table deepens the unsaturated zone, makes the flow paths disconnected and decreases the overall head gradients. This causes the ET-induced diel signals to move relatively slow toward the stream network.

The shortest lag times of 2–3 h are observed for very low flow (<2 m^3/h) in the events in February and March. These short lag times for low flows suggest that a very small portion of the riparian area near the stream contributes to the streamflow through the hyporheic exchange. Therefore, any change in the ET rate more rapidly impacts the streamflow at the outlet. Moreover, March was observed as the last month with flows showing diurnal fluctuations, which suggests that the diel fluctuations started to disappear at the beginning of autumn.

5 | CONCLUSIONS

This study developed a new method to estimate riparian ET by analysing the streamflow response to diurnal ET. It is assumed that the daily flow fluctuations occur because of the ET differences between day and night. The new method estimates a temporal variation of the active riparian area during a flood recession by assuming a linear correlation between groundwater storage and active riparian area. The estimated riparian ET from the new method shows an acceptable correlation with the hourly PET calculated from FAO 56. The method provides a better understanding of the impact of the riparian zone on streamflow patterns. In addition, the new method requires fewer experimental parameters to estimate ET abstracted from riparian zone than the calculation of PET from conventional methods, for example, FAO 56. Moreover, PET is used as a reference to optimize the riparian ET and estimates the active riparian area at the beginning of the recession. However, if a reliable discharge-area relationship is available from field investigation or another procedure, the daily fluctuations in streamflow can predict riparian ET values without needing PET as a reference.

ACKNOWLEDGEMENTS

The authors of the paper would like to thank Lincoln Agritech Ltd. for providing flow and weather data. Open access publishing facilitated by University of Waikato, as part of the Wiley - University of Waikato agreement via the Council of Australian University Librarians.

DATA AVAILABILITY STATEMENT

The corresponding author's data supporting this study's findings are available via the following link. The data that support the findings of this study are available from the corresponding author.

ORCID

Ali Shokri https://orcid.org/0000-0001-9482-8105

REFERENCES

Allen, R. G., & Pereira, L. S. (1991). FAO irrigation and drainage paper no 56. *Applied Ocean Research*, *13*, 110–115. https://doi.org/10.1016/S0141-1187(05)80058-6

Barnard, H. R., Graham, C. B., van Verseveld, W. J., Brooks, J. R., Bond, B. J., & McDonnell, J. J. (2010). Mechanistic assessment of hillslope transpiration controls of diel subsurface flow: A steady-state irrigation approach. *Ecohydrology*, *3*, 133–142. https://doi.org/10.1002/eco.114

Bond, B. J., Jones, J. A., Moore, G., Phillips, N., Post, D., & McDonnell, J. J. (2002). The zone of vegetation influence on baseflow revealed by diel patterns of streamflow and vegetation water use in a headwater basin. *Hydrological Processes*, *16*(8), 1671–1677. https://doi.org/10.1002/hyp.5022

Boronina, A., Golubev, S., & Balderer, W. (2005). Estimation of actual evapotranspiration from an alluvial aquifer of the Kouris catchment (Cyprus) using continuous streamflow records. *Hydrological Processes*, *19*(20), 4055–4068. https://doi.org/10.1002/hyp.5871

Brunner, P., Cook, P. G., & Simmons, C. T. (2009). Hydrogeologic controls on disconnection between surface water and groundwater. *Water Resources Research*, *45*(1), W01422. https://doi.org/10.1029/2008WR006953

Brunner, P., Li, H. T., Kinzelbach, W., Li, W. P., & Dong, X. G. (2008). Extracting phreatic evaporation from remotely sensed maps of evapotranspiration. *Water Resources Research*, *44*(8), W08428. https://doi.org/10.1029/2007WR006063

Burt, T. P. (1979). Diurnal variations in stream discharge and throughflow during a period of low flow. *Journal of Hydrology*, *41*(3–4), 291–301. https://doi.org/10.1016/0022-1694(79)90067-2

Cadol, D., Kampf, S., & Wohl, E. (2012). Effects of evapotranspiration on baseflow in a tropical headwater catchment. *Journal of Hydrology*, *462–463*, 4–14. https://doi.org/10.1016/j.jhydrol.2012.04.060

Dolan, T. J., Hermann, A. J., Bayley, S. E., & Zoltek, J. (1984). Evapotranspiration of a Florida, U.S.A., freshwater wetland. *Journal of Hydrology*, *74*(3–4), 355–371. https://doi.org/10.1016/0022-1694(84)90024-6

Dufour S., Rodríguez-González P.M. (2019). Riparian zone/riparian vegetation definition: principles and recommendations. Report, COST Action

CA16208 CONVERGES, 20 pp. https://converges.eu/resources/riparian-zone-riparian-vegetation-definition-principles-and-recommendations/.

Fahle, M., & Dietrich, O. (2014). Estimation of evapotranspiration using diurnal groundwater level fluctuations: Comparison of different approaches with groundwater lysimeter data. *Water Resources Research*, *50*(1), 273–286. https://doi.org/10.1002/2013WR014472

Fenicia, F., Savenije, H. H. G., Matgen, P., & Pfister, L. (2006). Is the groundwater reservoir linear? Learning from data in hydrological modelling. *Hydrology and Earth System Sciences*, *10*(1), 139–150. https://doi.org/10.5194/hess-10-139-2006

Geisler, E. T. (2016). Riparian zone evapotranspiration using streamflow diel signals. *Boise State University Theses and Dissertations*, Master of Science in Hydrologic Sciences. https://scholarworks.boisestate.edu/td/1090

Goodrich, D. C., Scott, R., Qi, J., Goff, B., Unkrich, C. L., Moran, M. S., Williams, D., Schaeffer, S., Snyder, K., MacNish, R., Maddock, T., Pool, D., Chehbouni, A., Cooper, D. I., Eichinger, W. E., Shuttleworth, W. J., Kerr, Y., Marsett, R., & Ni, W. (2000). Seasonal estimates of riparian evapotranspiration using remote and in situ measurements. *Agricultural and Forest Meteorology*, *105*(1–3), 281–309. https://doi.org/10.1016/S0168-1923(00)00197-0

Graham, C. B., Barnard, H. R., Kavanagh, K. L., & Mcnamara, J. P. (2012). Catchment scale controls the temporal connection of transpiration and diel fluctuations in stream flow, https://doi.org/10.1002/hyp

Gribovszki, Z., Kalicz, P., Kucsara, M., Szilágyi, J., & Vig, P. (2008). Evapotranspiration calculation on the basis of the riparian zone water balance. Acta Silvatica et Lignaria Hungarica.

Gribovszki, Z., Kalicz, P., Szilágyi, J., & Kucsara, M. (2008). Riparian zone evapotranspiration estimation from diurnal groundwater level fluctuations. *Journal of Hydrology*, *349*(1–2), 6–17. https://doi.org/10.1016/j.jhydrol.2007.10.049

Gribovszki, Z., Szilágyi, J., & Kalicz, P. (2010). Diurnal fluctuations in shallow groundwater levels and streamflow rates and their interpretation - a review. *Journal of Hydrology*, *385*(1–4), 371–383. https://doi.org/10.1016/j.jhydrol.2010.02.001

Gupta, H. v., Kling, H., Yilmaz, K. K., & Martinez, G. F. (2009). Decomposition of the mean squared error and NSE performance criteria: Implications for improving hydrological modelling. *Journal of Hydrology*, *377*, 80–91. https://doi.org/10.1016/j.jhydrol.2009.08.003

Johnson, B., Malama, B., Barrash, W., & Flores, A. N. (2013). Recognising and modeling variable drawdown due to evapotranspiration in a semi-arid riparian zone considering local differences in vegetation and distance from a river source. *Water Resources Research*, *49*, 1030–1039. https://doi.org/10.1002/wrcr.20122

Kellogg, D. Q., Gold, A. J., Groffman, P. M., Stolt, M. H., & Addy, K. (2008). Riparian ground-water flow patterns using Flownet analysis: Evapotranspiration-induced upwelling and implications for N removal 1. *JAWRA Journal of the American Water Resources Association*, *44*(4), 1024–1034. https://doi.org/10.1111/j.1752-1688.2008.00218.x

Kirchner, J. W. (2009). Catchments as simple dynamical systems: Catchment characterisation, rainfall-runoff modeling, and doing hydrology backward. *Water Resources Research*, *45*(2), W02429. https://doi.org/10.1029/2008WR006912

Kirchner, J. W., Godsey, S. E., Solomon, M., Osterhuber, R., McConnell, J. R., & Penna, D. (2020). The pulse of a montane ecosystem: Coupling between daily cycles in solar flux, snowmelt, transpiration, groundwater, and streamflow at Sagehen Creek and Independence Creek, Sierra Nevada, USA. *Hydrology and Earth System Sciences*, *24*(11), 5095–5123. https://doi.org/10.5194/hess-24-5095-2020

Lascano, R. J., Goebel, T. S., Booker, J., Baker, J. T., & Gitz, D. C., III. (2016). The stem heat balance method to measure transpiration: Evaluation of a new sensor. *Agricultural Sciences*, *07*, 604–620. https://doi.org/10.4236/as.2016.79057

Loheide, S. P., II. (2008). A method for estimating subdaily evapotranspiration of shallow groundwater using diurnal water table fluctuations. *Ecohydrology*, *1*(1), 59–66. https://doi.org/10.1002/eco.7

Loheide, S. P., Butler, J. J., & Gorelick, S. M. (2005). Estimation of groundwater consumption by phreatophytes using diurnal water table fluctuations: A saturated-unsaturated flow assessment. *Water Resources Research*, *41*(7), 1–14. https://doi.org/10.1029/2005WR003942

Lundquist, J. D., & Cayan, D. R. (2002). Seasonal and spatial patterns in diurnal cycles in streamflow in the Western United States. *Journal of Hydrometeorology*, *3*(5), 591–603.

Lyne, V. D., & Hollick, M. (1979). Stochastic time-variable rainfall-runoff modelling. Institute of Engineers Australia National Conference.

Martí, E., Fisher, S. G., Schade, J. D., & Grimm, N. B. (2000). Flood frequency and stream–riparian linkages in arid lands. In *Streams and ground waters* (pp. 111–136). Elsevier. https://doi.org/10.1016/B978-012389845-6/50005-3

Müller, K., Srinivasan, M. S., Trolove, M., & McDowell, R. W. (2010). Identifying and linking source areas of flow and P transport in dairy-grazed headwater catchments, North Island, New Zealand. *Hydrological Processes*, *24*, 3689–3705. https://doi.org/10.1002/hyp.7809

Nachabe, M., Shah, N., Ross, M., & Vomacka, J. (2005). Evapotranspiration of two vegetation covers in a shallow water table environment. *Soil Science Society of America Journal*, *69*(2), 492–499. https://doi.org/10.2136/sssaj2005.0492

Pronger, J., Campbell, D. I., Clearwater, M. J., Rutledge, S., Wall, A. M., & Schipper, L. A. (2016). Low spatial and inter-annual variability of evaporation from a year-round intensively grazed temperate pasture system. *Agriculture, Ecosystems & Environment*, *232*, 46–58. https://doi.org/10.1016/j.agee.2016.07.011

Reigner, I. C. (1966). A method of estimating streamflow loss by evapotranspiration from the riparian zone. *Forest Science*, *12*(2), 130–139. https://doi.org/10.1093/forestscience/12.2.130

Rugenski, A. T., Minshall, G. W., Hauer, F. R. (2017). Riparian Processes and Interactions. In *Methods in Stream Ecology* (pp. 83–111). Elsevier. https://doi.org/10.1016/B978-0-12-813047-6.00006-1

Satchithanantham, S., Wilson, H. F., & Glenn, A. J. (2017). Contrasting patterns of groundwater evapotranspiration in grass and tree dominated riparian zones of a temperate agricultural catchment. *Journal of Hydrology*, *549*, 654–666. https://doi.org/10.1016/j.jhydrol.2017.04.016

Schwab, M., Klaus, J., Pfister, L., & Weiler, M. (2016). Diel discharge cycles explained through viscosity fluctuations in riparian inflow. *Water Resources Research*, *52*(11), 8744–8755. https://doi.org/10.1002/2016WR018626

Scotter, D., & Heng, L. (2003). Estimating reference crop evapotranspiration in NewZealand. *Journal of Hydrology (New Zealand)*, *42*, 1–10.

Sumargo, E., & Cayan, D. R. (2018). The influence of cloudiness on hydrologic fluctuations in the mountains of the western United States. *Water Resources Research*, *54*, 8478– 8499.

Spence, C., & Mengistu, S. G. (2019). On the relationship between flood and contributing area. *Hydrological Processes*, *33*(14), 1980–1992. https://doi.org/10.1002/hyp.13467

Széles, B., Broer, M., Parajka, J., Hogan, P., Eder, A., Strauss, P., & Blöschl, G. (2018). Separation of scales in transpiration effects on low flows: A spatial analysis in the hydrological open air laboratory. *Water Resources Research*, *54*(9), 6168–6188. https://doi.org/10.1029/2017WR022037

Szilagyi, J., Gribovszki, Z., & Kalicz, P. (2007). Estimation of catchment-scale evapotranspiration from baseflow recession data: Numerical model and practical application results. *Journal of Hydrology*, *336*(1–2), 206–217. https://doi.org/10.1016/j.jhydrol.2007.01.004

Tallaksen, L. M. (1995). A review of baseflow recession analysis. *Journal of Hydrology*, *165*(1–4), 349–370. https://doi.org/10.1016/0022-1694(94)02540-R

Troxell, H. C. (1936). The diurnal fluctuation in the groundwater and flow of the Santa Ana river and its meaning. *Transactions, American Geophysical Union*, *17*(2), 496. https://doi.org/10.1029/TR017i002p00496

Tschinkel, H. M. (1963). Short-term fluctuation in streamflow as related to evaporation and transpiration. *Journal of Geophysical Research*, *68*(24), 6459–6469.

White, W. N. (1932). A method of estimating groundwater supplies based on discharge by plants and evaporation from soil: Results of investigations in Escalante Valley, Utah. Water Supply Paper (659th ed., 659). US Geological Survey. http://doi.org/10.3133/wsp659A

Wilcock, R. J., Monaghan, R. M., Quinn, J. M., Campbell, A. M., Thorrold, B. S., Duncan, M. J., McGowan, A. W., & Betteridge, K. (2006). Land-use impacts and water quality targets in the intensive dairying catchment of the Toenepi stream, New Zealand. *New Zealand Journal of Marine and Freshwater Research*, *40*(1), 123–140. https://doi.org/10.1080/00288330.2006.9517407

Woodward, S. J. R., Stenger, R., & Bidwell, V. J. (2013). Dynamic analysis of stream flow and water chemistry to infer subsurface water and nitrate fluxes in a lowland dairying catchment. *Journal of Hydrology*, *505*, 299–311. https://doi.org/10.1016/j.jhydrol.2013.07.044

How to cite this article: Sarwar, M. W., Campbell, D. I., & Shokri, A. (2022). Riparian zone as a variable source area for the estimation of evapotranspiration through the analysis of daily fluctuations in streamflow. *Hydrological Processes*, *36*(10), e14708. https://doi.org/10.1002/hyp.14708

APPENDIX A

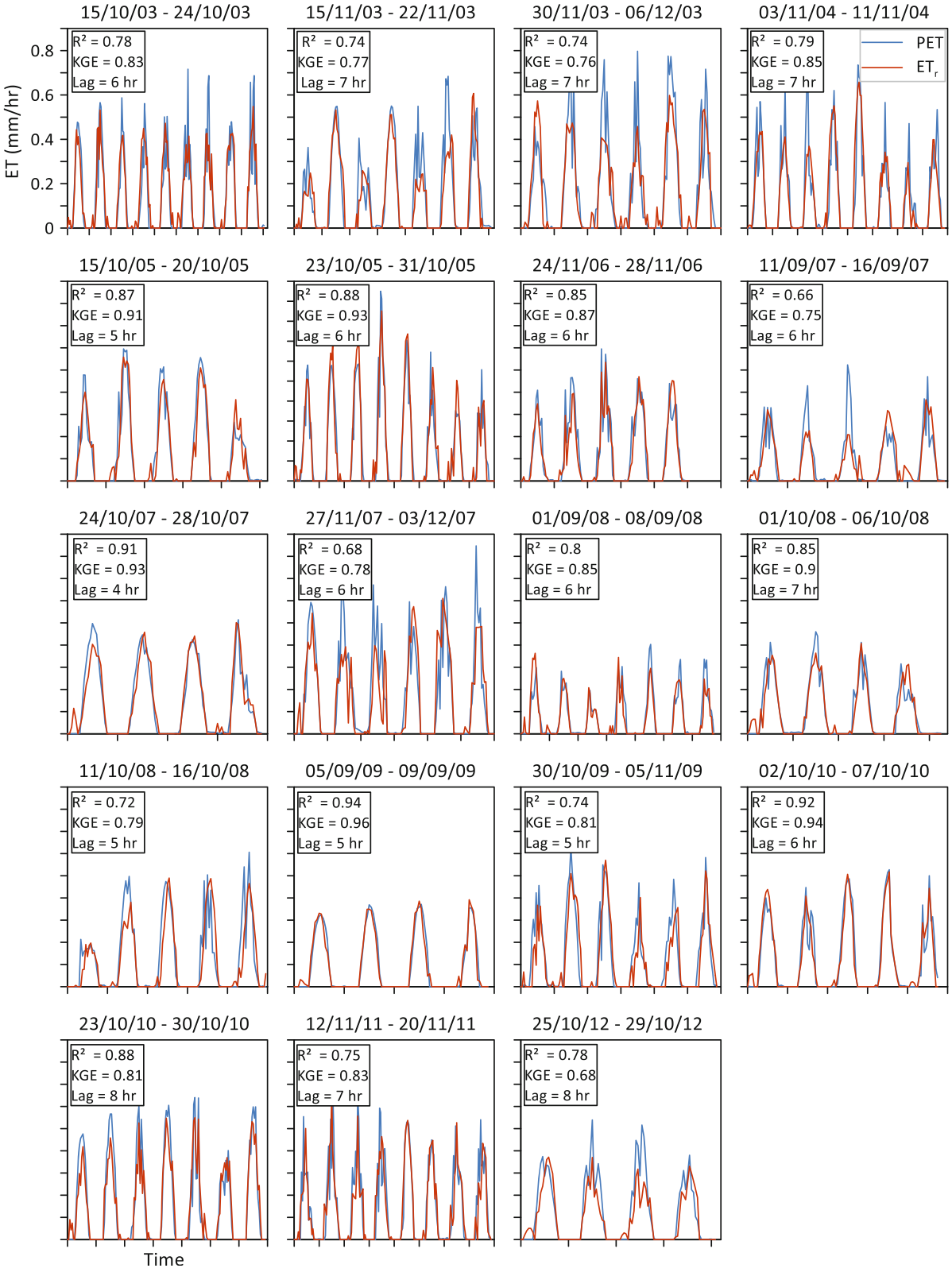

FIGURE A1 A comparison between hourly PET estimated by FAO 56 and ET_r estimated by the new method during spring months (September–October–November)

APPENDIX B

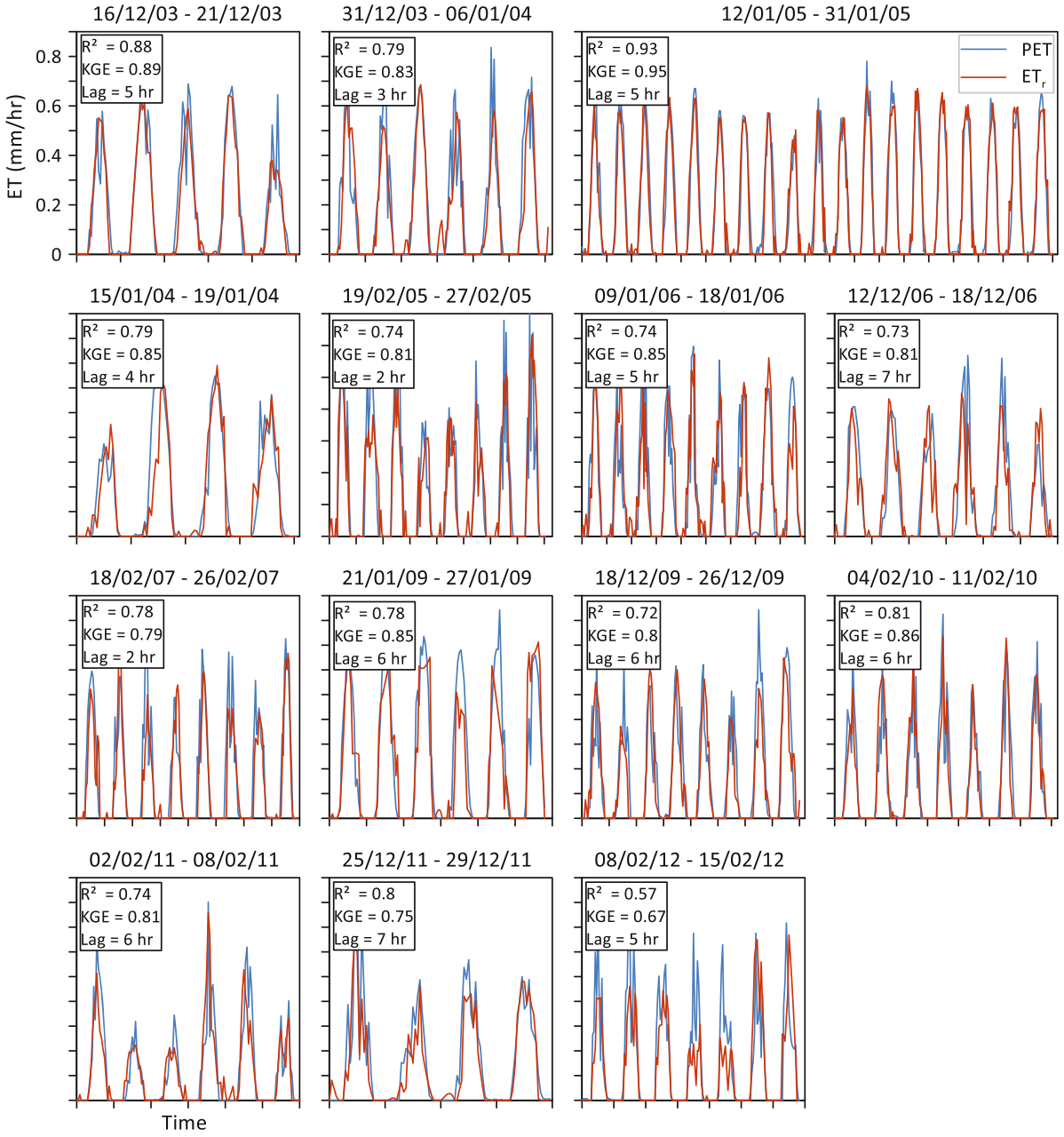

FIGURE A2 A comparison between hourly PET estimated by FAO 56 and ET_r estimated by the new method during the summer months (December–January–February)

APPENDIX C

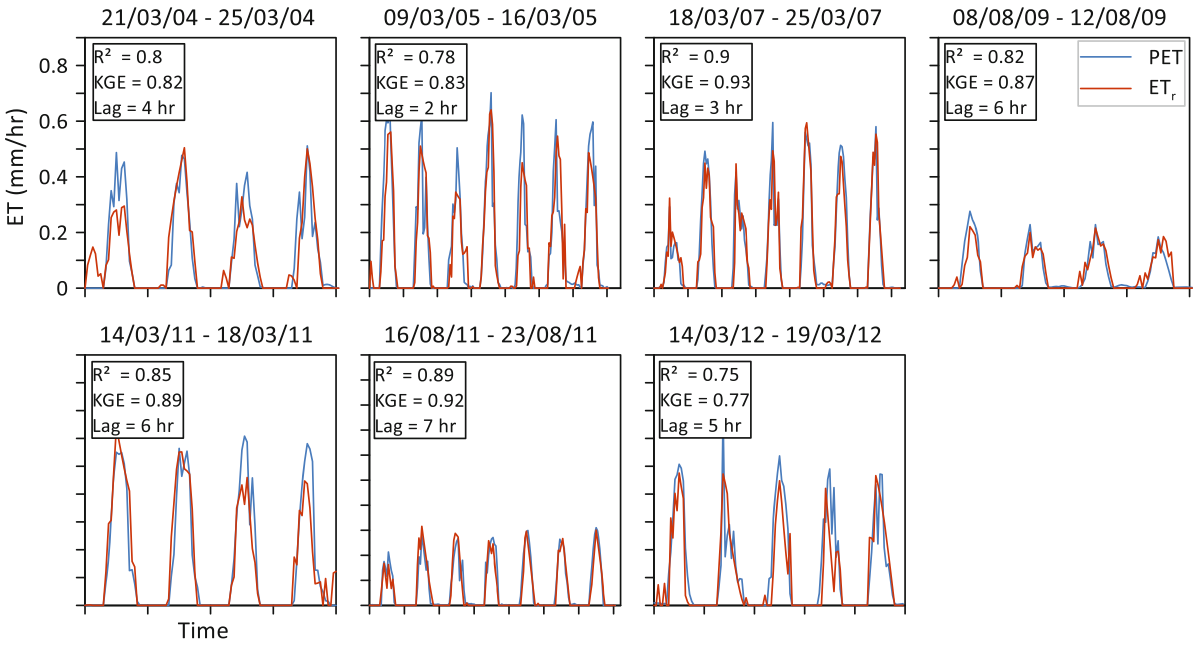

FIGURE A3 A comparison between hourly PET estimated by FAO 56 and ET_r estimated by the new method during the winter (August) and early autumn (March) months.